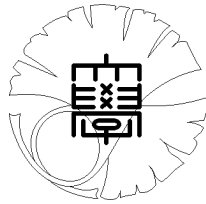


UTMS 2008–21

July 25, 2008

**Discontinuous Galerkin FEM
of Hybrid displacement type
– Development of polygonal elements –**
by
Fumio KIKUCHI, Keizo ISHII
and Issei OIKAWA



UNIVERSITY OF TOKYO

GRADUATE SCHOOL OF MATHEMATICAL SCIENCES

KOMABA, TOKYO, JAPAN

Discontinuous Galerkin FEM of Hybrid Displacement Type – Development of Polygonal Elements –

Fumio KIKUCHI*, Keizo ISHII** and Issei OIKAWA*

* *Graduate School of Mathematical Sciences, University of Tokyo,
3-8-1 Komaba, Meguro, Tokyo, 153-8914 Japan.*

** *Quint Corporation, 1-14-1 Fuchu-cho, Fuchu, Tokyo, 183-0055, Japan.*

Abstract

As a discontinuous Galerkin FEM, we propose a formulation based on Tong's hybrid displacement method and the stabilization technique, and develop polygonal elements for linear static plane stress problems. The basic ideas are the introduction of inter-element displacements and the use of stabilization terms. Here we only present polygonal elements with polynomial approximation functions. That is, we employ discontinuous linear polynomial fields for element displacements, while we adopt continuous piecewise linear polynomial fields for inter-element displacements. By static condensation, we can also obtain the usual element stiffness matrices and the element load vectors for nodal inter-element edge displacements, so that our elements can be easily built into various existing FEM codes and even mixed use with conventional elements is possible. We obtain some numerical results to show the validity of our approach and also to see the influence of the stabilization parameter size and the flexibility in element shape.

Key Words: FEM, Discontinuous Galerkin method, Hybrid displacement method, Polygonal element, Plane stress problem.

Mathematical Subject Classification 2000: 65N30, 74S05.

1. INTRODUCTION

Recently, considerable attention has been drawn to the discontinuous Galerkin FEM or DGFEM^{1,2,3}), whose root is reported to be in the neutron transport problems. In this approach, the continuity of the approximate functions is not required before-hand, but is dealt with by the Lagrange multiplier method and/or the penalty method. Compared with the classical FEM, a merit of such an approach is that much wider class of approximate functions become available, so that the usual Cartesian polynomials can be used for finite elements of more general shapes, and various singularity functions can be also incorporated into the approximate functions to capture singularities caused by e.g. cracks. On the other hand, depending on the methods of dealing with the inter-element discontinuity, the sizes and band-widths of the arising linear simultaneous equations may become much larger than those of the conventional FEM.

Actually, the root can be also traced to solid mechanics: the well-known non-conforming and hybrid FEM's use discontinuous functions as approximate displacement fields. Typical examples are Pian's hybrid stress method⁴) and Tong's hybrid displacement one⁵), and they are often called FEM's with relaxed continuity requirements. One of the authors also developed a variant of the hybrid displacement one and applied it to plate and shell problems^{6,7}) with numerical results. Unfortunately, our trial was only partial success because of lack of effective stabilization techniques. However, this approach has the merit that we can obtain the element stiffness matrices and element load vectors similar to those of the conventional FEM.

Stimulated by rapid development of DGFEM, the authors now try to propose a hybrid displacement approach by stabilizing our old method. We will show the idea by using the plane stress problem as a model problem, and then give some concrete finite element models of polygonal shape. Moreover, some numerical results are given to show the effectiveness of the proposed finite elements. A closely related but different approach is also proposed as HPM⁸).

2. LINEAR PLANE STRESS PROBLEM

We will summarize the linear static plane stress problem in the isotropic case⁹). Although we can deal with more general three-dimensional cases, we consider the above restricted case for simplicity. Let us introduce the orthogonal Cartesian coordinates into the space which contains a thin plate-like elastic body, and denote the point by $\mathbf{x} = (x_i)$, where i ranges from 1 to 3. However, in the plane stress problem, the independent variables are essentially x_1 and x_2 only, while x_3 is used as a subsidiary coordinate component. We will often use (x, y) instead of (x_1, x_2) . The thickness of the plate-like body is denoted by t , which can be a function of (x, y) .

First, for the two-dimensional displacement vector $\mathbf{u} = (u_i)_{i=1,2}$ of the elastic body, the (linearized) strain tensor $\varepsilon_{ij} = \varepsilon_{ij}(\mathbf{u})$ is given by

$$\varepsilon_{ij}(\mathbf{u}) = \frac{1}{2}(\partial u_i / \partial x_j + \partial u_j / \partial x_i) \quad ; \quad 1 \leq i, j \leq 2. \quad (1)$$

Instead of the strain tensor, we will mainly use its engineering expression of vector form :

$$\boldsymbol{\varepsilon} = \boldsymbol{\varepsilon}(\mathbf{u}) = \begin{pmatrix} \varepsilon_x \\ \varepsilon_y \\ \gamma_{xy} \end{pmatrix} = \begin{pmatrix} \varepsilon_{11} \\ \varepsilon_{22} \\ 2\varepsilon_{12} \end{pmatrix}. \quad (2)$$

We also use the engineering stress components in vector expression :

$$\boldsymbol{\sigma} = \begin{pmatrix} \sigma_x \\ \sigma_y \\ \tau_{xy} \end{pmatrix} = \begin{pmatrix} \sigma_{11} \\ \sigma_{22} \\ \sigma_{12} = \sigma_{21} \end{pmatrix}, \quad (3)$$

where σ_{11} etc. denote the usual tensor expressions for the stresses.

To describe the isotropic linear elastic stress-strain relation, let us introduce the matrix D :

$$D = \frac{E}{1 - \nu^2} \begin{bmatrix} 1 & \nu & 0 \\ \nu & 1 & 0 \\ 0 & 0 & \frac{1-\nu}{2} \end{bmatrix}, \quad (4)$$

where E is Young's modulus and ν Poisson's ratio. Usually, we assume that $E > 0$ and $0 < \nu < 1/2$. Then the stress-strain relation is written by

$$\boldsymbol{\sigma} = D\boldsymbol{\varepsilon}. \quad (5)$$

Furthermore, we assume that the distributed external body force $\mathbf{f} = (f_i)_{i=1,2}$ is applied to the elastic body. Here, \mathbf{f} has the dimension of force per unit in-plane area, so that the factor t is already multiplied to the corresponding volume force.

On the boundary $\Gamma = \partial\Omega$ of the two-dimensional domain Ω for the elastic body, we impose the following geometric and kinetic boundary conditions in order :

$$\mathbf{u} = \mathbf{g}_1 \text{ on } \Gamma_1, \quad \mathbf{s} = \mathbf{g}_2 \text{ on } \Gamma_2, \quad (6)$$

where Γ_1 and Γ_2 are two disjoint parts dividing Γ , $\mathbf{g}_1 = (g_{1i})_{i=1,2}$ and $\mathbf{g}_2 = (g_{2i})_{i=1,2}$ are vector-valued functions defined on Γ_1 and Γ_2 , respectively, and $\mathbf{s} = (s_i)_{i=1,2}$ is the surface traction force vector per unit length of the boundary. It holds for $\mathbf{s} = (s_i)$ and $\boldsymbol{\sigma}$ the relation : $s_i = t \sum_{j=1}^2 \sigma_{ij} n_j$, where $\mathbf{n} = (n_i)_{i=1,2}$ is the unit outward normal vector on Γ .

Now the functional $\Pi_0[\mathbf{u}]$ employed in the principle of minimum potential energy is given by

$$\Pi_0[\mathbf{u}] = \iint_{\Omega} \left(\frac{t}{2} \boldsymbol{\varepsilon}(\mathbf{u})^T D \boldsymbol{\varepsilon}(\mathbf{u}) - \mathbf{u}^T \mathbf{f} \right) dx dy - \int_{\Gamma_2} \mathbf{u}^T \mathbf{g}_2 d\gamma, \quad (7)$$

where “ T ” denotes the transpose operator, $d\gamma$ the line element on Γ , and the independent argument function is the displacement \mathbf{u} only, which we require to satisfy the first boundary condition in (6). Notice that the factor t comes from the integration in the x_3 -direction.

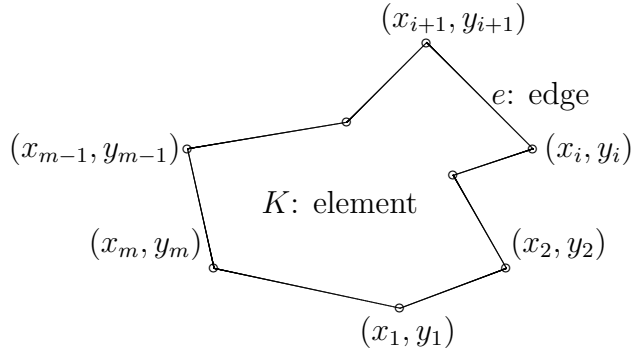


Fig. 1 m -polygonal element K

3. VARIATIONAL FUNCTIONAL FOR DISCONTINUOUS GALERKIN FEM

Here we give statements for the plane stress problem. In the proposed discontinuous Galerkin FEM of hybrid displacement type, we consider the case where Ω is a bounded polygonal domain for the moment. Otherwise, we need to approximate the original domain by a polygonal one. Then we introduce subdivision \mathcal{T}^h of Ω by a finite number of polygonal finite elements. Each finite element $K \in \mathcal{T}^h$ (or element in short) is an m polygonal domain (Fig. 1), where $m \geq 3$ is an integer and can differ with K , but is bounded from above independently of \mathcal{T}^h . We also assume that K is not too ‘thin’. Thus the boundary ∂K of a representative element $K \in \mathcal{T}^h$ consists of m edges, each of which is denoted by e ($\subset \partial K$) with $|e|$ = length of e . Moreover, we assume that ∂K does not intersect with itself. The diameter and area of K is denoted by h_K and $|K|$, respectively, and we also define the discretization parameter h for \mathcal{T}^h by $h := \max_{K \in \mathcal{T}^h} h_K$ when we discuss the convergence of the finite element solutions by mesh refinement.

In Tong’s hybrid displacement method⁵⁾, we use the interelement displacement field $\hat{\mathbf{u}}$ and the element boundary traction field \mathbf{s} as the arguments besides the element-wise displacement field \mathbf{u} . We permit \mathbf{u} of an element to be independent of those of other elements and to be discontinuous across interelement boundaries, while $\hat{\mathbf{u}}$ is defined on the interfaces of the elements and is single-valued on each edge shared by two adjacent elements. On the other hand, \mathbf{s} is also defined on edges of elements but does not need to be common to two adjacent elements. Then the original variational functional of Tong in the linear plane stress case is given by

$$\Pi_1[\mathbf{u}, \hat{\mathbf{u}}, \mathbf{s}] = \sum_{K \in \mathcal{T}^h} \left\{ \iint_K \left(\frac{t}{2} \boldsymbol{\varepsilon}(\mathbf{u})^T D \boldsymbol{\varepsilon}(\mathbf{u}) - \mathbf{u}^T \mathbf{f} \right) dx dy - \int_{\Gamma_2} \hat{\mathbf{u}}^T \mathbf{g}_2 d\gamma + \int_{\partial K} \mathbf{s}^T (\hat{\mathbf{u}} - \mathbf{u}) d\gamma \right\}, \quad (8)$$

where we assume that

$$\hat{\mathbf{u}} = \mathbf{g}_1 \quad \text{on } \Gamma_1. \quad (9)$$

In the simplified hybrid method of Kikuchi-Ando^{6,7)}, \mathbf{s} on ∂K is eliminated by using \mathbf{u} of the associated K as well as the relations $\boldsymbol{\sigma} = D\boldsymbol{\varepsilon}(\mathbf{u})$ and $s_i = t \sum_{j=1}^2 \sigma_{ij} n_j$ ($i = 1, 2$), so that \mathbf{s} is no longer an independent argument of the functional. If necessary, such an \mathbf{s} is denoted by $\mathbf{s}(\mathbf{u})$.

In the proposed discontinuous Galerkin method of hybrid displacement type, the above simplified functional is augmented with stabilization (or penalization) terms as follows:

$$\begin{aligned} \Pi_2[\mathbf{u}, \hat{\mathbf{u}}] = & \sum_K \left\{ \iint_K \left(\frac{t}{2} \boldsymbol{\varepsilon}(\mathbf{u})^T D \boldsymbol{\varepsilon}(\mathbf{u}) - \mathbf{u}^T \mathbf{f} \right) dx dy - \int_{\Gamma_2} \mathbf{g}_2^T \hat{\mathbf{u}} d\gamma \right. \\ & \left. + \int_{\partial K} \mathbf{s}(\mathbf{u})^T (\hat{\mathbf{u}} - \mathbf{u}) d\gamma + \sum_{e \subset \partial K} \frac{\eta_{K,e}}{2h_{K,e}} \int_e (\mathbf{u} - \hat{\mathbf{u}})^T (\mathbf{u} - \hat{\mathbf{u}}) d\gamma \right\}, \end{aligned} \quad (10)$$

where $\eta_{K,e} > 0$ is the stabilization parameter for each edge $e \subset \partial K$, and $h_{K,e}$ is the length parameter for e such as the edge length $|e|$ itself, $|K|/|e|$ etc. Moreover, we impose the same condition on $\hat{\mathbf{u}}$ as in (9). The present variational principle is in general a stationary one, but can become an minimum one under appropriate conditions on the stabilization parameters¹⁾.

4. POLYGONAL LINEAR ELEMENT

Using the variational functional Π_2 , let us develop a finite element for the linear plane stress problems. For simplicity, we assume that the material corresponding to each element is isotropic and homogeneous, and the element thickness is also constant. That is, E , ν and t of each K are constant functions of (x, y) . As approximations to the two displacement fields \mathbf{u} and $\hat{\mathbf{u}}$, we not only can use polynomial functions of various degrees, but also more general analytic functions. For simplicity, we here show the use of piecewise linear polynomials only as a concrete example. On the other hand, we consider general m -polygonal sub-domains as finite elements.

4.1 Approximate displacements

First, the approximation \mathbf{u}_h of \mathbf{u} in element K is chosen to be linear and is completely independent of those in other elements. Thus such a \mathbf{u}_h is a discontinuous piecewise linear polynomial over the finite element subdivision \mathcal{T}^h . For a triangular element, it is possible to express \mathbf{u}_h by the interpolation form with the vertices or midpoints of K taken as nodes. But even in this case, the continuity of \mathbf{u}_h at nodes shared with other elements is never imposed unlike the conventional finite elements. For elements of other shapes, it is impossible to employ whole vertices as nodes. Thus it is natural to express \mathbf{u}_h in the node-free form for each K :

$$\mathbf{u}_h(x, y) = \begin{pmatrix} u_{1h}(x, y) \\ u_{2h}(x, y) \end{pmatrix} = \begin{pmatrix} \alpha_1 + \alpha_2 x + \alpha_3 y \\ \alpha_4 + \alpha_5 x + \alpha_6 y \end{pmatrix} = N_1(x, y) \boldsymbol{\alpha}, \quad (11)$$

$$\boldsymbol{\alpha} = (\alpha_1, \dots, \alpha_6)^T \quad (\alpha_1, \dots, \alpha_6 \text{ are coefficients}), \quad N_1(x, y) = \begin{bmatrix} 1 & x & y & 0 & 0 & 0 \\ 0 & 0 & 0 & 1 & x & y \end{bmatrix}. \quad (12)$$

Of course we can introduce translations and scalings to (x, y) . Using the linear coordinate ξ on $e \subset \partial K$ and a 2×6 matrix function $N_2(\xi)$ derived from $N_1(x, y)$, \mathbf{u}_h on e can be expressed as

$$\mathbf{u}_h(\xi) = N_2(\xi) \boldsymbol{\alpha}; \quad 0 \leq \xi \leq |e|. \quad (13)$$

Secondly, the approximate function $\hat{\mathbf{u}}_h$ for $\hat{\mathbf{u}}$ is assumed to be linear on each edge e of finite elements and is common to any two adjacent elements sharing e . On the ends of e , i.e., at the vertices of elements, we can either impose or disregard the continuity on $\hat{\mathbf{u}}_h$, but we will only consider the continuous case to reduce the number of unknowns. Thus $\hat{\mathbf{u}}_h$ can be expressed as a continuous piecewise linear polynomial over the graph composed of vertices and edges in \mathcal{T}^h , and also as an interpolation function in terms of vertex values of $\hat{\mathbf{u}}_h$. Then the vertices play the role of nodes as in the classical FEM. We also assume that $\hat{\mathbf{u}}_h$ takes the value of \mathbf{g}_1 at the vertices on Γ_1 to approximate (9). Using ξ on $e \subset \partial K$, we can express $\hat{\mathbf{u}}_h$ as

$$\hat{\mathbf{u}}_h(\xi) = \begin{pmatrix} \hat{u}_{1h}(\xi) \\ \hat{u}_{2h}(\xi) \end{pmatrix} = \begin{pmatrix} \beta_1 + \beta_2\xi \\ \beta_3 + \beta_4\xi \end{pmatrix} \quad (\beta_1, \dots, \beta_4 \text{ are coefficients}). \quad (14)$$

The above $\hat{\mathbf{u}}_h(\xi)$ can be also expressed in terms of the $2m$ -dimensional vector \mathbf{U} composed of its values at all m vertices:

$$\hat{\mathbf{u}}_h(\xi) = N_3(\xi)\mathbf{U}; \quad 0 \leq \xi \leq |e|, \quad (15)$$

where $N_3(\xi)$ is a $2 \times 2m$ matrix function of ξ usually with many zero entries.

4.2 Derivation of element matrices and vectors

Using (1), (2) and (11), the approximate strain vector $\boldsymbol{\varepsilon}_h = \boldsymbol{\varepsilon}(\mathbf{u}_h)$ in each K is given by

$$\boldsymbol{\varepsilon}_h = \begin{pmatrix} \varepsilon_{xh} \\ \varepsilon_{yh} \\ \gamma_{xyh} \end{pmatrix} = M_1\boldsymbol{\alpha}; \quad M_1 = \begin{bmatrix} 0 & 1 & 0 & 0 & 0 & 0 \\ 0 & 0 & 0 & 0 & 0 & 1 \\ 0 & 0 & 1 & 0 & 1 & 0 \end{bmatrix}. \quad (16)$$

Then the element strain energy for the assumed \mathbf{u}_h is calculated as

$$\iint_K \frac{t}{2} \boldsymbol{\varepsilon}(\mathbf{u}_h)^T D \boldsymbol{\varepsilon}(\mathbf{u}_h) dx dy = \frac{t|K|}{2} \boldsymbol{\alpha}^T M_1^T D M_1 \boldsymbol{\alpha}, \quad (17)$$

where $|K|$, the area of K , is concretely calculated as follows by using vertices $(x_i, y_i)_{1 \leq i \leq m}$ of K arranged in the anti-clockwise order:

$$|K| = \frac{1}{2} \sum_{i=1}^m (x_i y_{i+1} - x_{i+1} y_i) \quad \text{with } (x_{m+1}, y_{m+1}) = (x_1, y_1). \quad (18)$$

For integrations of general polynomials in K , the use of the Stokes formula is effective^{4,9}.

We also need the approximate \mathbf{s}_h for \mathbf{s} on $e \subset \partial K$, which is derived from $\boldsymbol{\sigma}_h = D\boldsymbol{\varepsilon}_h$ as

$$\mathbf{s}_h = M_2\boldsymbol{\alpha}; \quad M_2 = t \begin{bmatrix} n_1 & 0 & n_2 \\ 0 & n_2 & n_1 \end{bmatrix} D M_1, \quad (19)$$

where $\mathbf{n} = (n_1, n_2)^T$ is the outward unit normal on e . Since ∂K is a polygon, \mathbf{n} is a constant vector on each e . Then the line integration $\int_{\partial K} \mathbf{s}(\mathbf{u})^T (\hat{\mathbf{u}} - \mathbf{u}) d\gamma$ in (10) with $\mathbf{s}(\mathbf{u}) = \mathbf{s}_h$, $\mathbf{u} = \mathbf{u}_h$

and $\hat{\mathbf{u}} = \hat{\mathbf{u}}_h$ can be performed easily by the mid-point rule on each e . That is, by using the value ξ^* of ξ at the mid-point of e as well as the edge length $|e|$, we have

$$\int_{\partial K} \mathbf{s}_h^T \hat{\mathbf{u}}_h d\gamma = \sum_{e \subset \partial K} |e| \boldsymbol{\alpha}^T M_2^T N_3(\xi^*) \mathbf{U}, \quad \int_{\partial K} \mathbf{s}_h^T \mathbf{u}_h d\gamma = \sum_{e \subset \partial K} |e| \boldsymbol{\alpha}^T M_2^T N_2(\xi^*) \boldsymbol{\alpha}. \quad (20)$$

Similarly, for the last term in (10), we obtain

$$\begin{aligned} \sum_{e \subset \partial K} \frac{\eta_{K,e}}{2h_{K,e}} \int_e (\mathbf{u}_h - \hat{\mathbf{u}}_h)^T (\mathbf{u}_h - \hat{\mathbf{u}}_h) d\gamma &= \sum_{e \subset \partial K} \frac{\eta_{K,e}}{2h_{K,e}} \left[\boldsymbol{\alpha}^T \int_0^{|e|} N_2^T(\xi) N_2(\xi) d\xi \boldsymbol{\alpha} \right. \\ &\quad \left. - 2\boldsymbol{\alpha}^T \int_0^{|e|} N_2^T(\xi) N_3(\xi) d\xi \mathbf{U} + \mathbf{U}^T \int_0^{|e|} N_3^T(\xi) N_3(\xi) d\xi \mathbf{U} \right], \end{aligned} \quad (21)$$

where the integrals can be performed by the Simpson formula or the two-point Gauss one⁴).

We should also consider the integrals related to \mathbf{f} and \mathbf{g}_2 . For each element K , we have

$$\iint_K \mathbf{u}_h^T \mathbf{f} dx dy = \boldsymbol{\alpha}^T \iint_K N_1^T(x, y) \mathbf{f}(x, y) dx dy. \quad (22)$$

If K has at least one edge contained to Γ_2 , we must consider the following line integral:

$$\sum_{e \subset \partial K \cap \Gamma_2} \int_e \hat{\mathbf{u}}_h^T \mathbf{g}_2 d\gamma = \mathbf{U}^T \sum_{e \subset \partial K \cap \Gamma_2} \int_0^{|e|} N_3^T(\xi) \mathbf{g}_2(\xi) d\xi. \quad (23)$$

Now the quantities in $\Pi_2(\mathbf{u}_h, \hat{\mathbf{u}}_h)$ related to K can be written as

$$\frac{1}{2} \boldsymbol{\alpha}^T A_{11} \boldsymbol{\alpha} + \boldsymbol{\alpha}^T A_{12} \mathbf{U} + \frac{1}{2} \mathbf{U}^T A_{22} \mathbf{U} - \boldsymbol{\alpha}^T \mathbf{F}_1 - \mathbf{U}^T \mathbf{F}_2, \quad (24)$$

where A_{11} and A_{22} are symmetric matrices, and the matrices and vectors are given by

$$\begin{aligned} A_{11} &= t|K| M_1^T D M_1 - \sum_{e \subset \partial K} |e| [M_2^T N_2(\xi^*) + N_2^T(\xi^*) M_2] + \sum_{e \subset \partial K} \frac{\eta_{K,e}}{h_{K,e}} \int_0^{|e|} N_2^T(\xi) N_2(\xi) d\xi, \\ A_{12} &= \sum_{e \subset \partial K} |e| M_2^T N_3(\xi^*) - \sum_{e \subset \partial K} \frac{\eta_{K,e}}{h_{K,e}} \int_0^{|e|} N_2^T(\xi) N_3(\xi) d\xi, \quad A_{22} = \sum_{e \subset \partial K} \frac{\eta_{K,e}}{h_{K,e}} \int_0^{|e|} N_3^T(\xi) N_3(\xi) d\xi, \\ \mathbf{F}_1 &= \iint_K N_1^T(x, y) \mathbf{f}(x, y) dx dy, \quad \mathbf{F}_2 = \sum_{e \subset \partial K \cap \Gamma_2} \int_0^{|e|} N_3^T(\xi) \mathbf{g}_2(\xi) d\xi. \end{aligned} \quad (25)$$

Since $\boldsymbol{\alpha}$ is independent of quantities related to all elements other than K , we can take variation (or derivative) of (24) with respect to $\boldsymbol{\alpha}$, and then equate the variation to zero. Then we find

$$A_{11} \boldsymbol{\alpha} + A_{12} \mathbf{U} - \mathbf{F}_1 = \mathbf{0}, \quad (26)$$

so that, if A_{11} is regular, we have $\boldsymbol{\alpha} = -A_{11}^{-1} A_{12} \mathbf{U} + A_{11}^{-1} \mathbf{F}_1$. Substituting this into (24), i.e., using a kind of static condensation process⁴, we obtain the expression in terms of \mathbf{U} only:

$$\frac{1}{2}\mathbf{U}^T A \mathbf{U} - \mathbf{U}^T \mathbf{F} - \frac{1}{2}\mathbf{F}_1^T A_{11}^{-1} \mathbf{F}_1; \quad A = A_{22} - A_{12}^T A_{11}^{-1} A_{12}, \quad \mathbf{F} = \mathbf{F}_2 - A_{12}^T A_{11}^{-1} \mathbf{F}_1. \quad (27)$$

From the above, we can find that A and \mathbf{F} correspond to the element stiffness matrix and the element load vector associated to the element nodal displacement vector \mathbf{U} for $\hat{\mathbf{u}}_h$. Thus we can use A and \mathbf{F} in completely the same fashion as in the conventional FEM, so that even the mixed use of the conventional elements and the present ones is available. Moreover, the use of m -polygonal elements with $m > 4$ and even non-convex elements is possible to a certain extent. Of course, too large m may yield loss of accuracy due to unbalanced approximation capabilities of \mathbf{u}_h and $\hat{\mathbf{u}}_h$. It is also to be noted that A and \mathbf{F} for the present triangular element coincide with those of the conventional linear triangular one. However, the internal displacement \mathbf{u}_h does not necessarily coincide with that of the conventional linear triangle, unless $\mathbf{F}_1 = \mathbf{0}$.

4.3 Stabilization parameter

The choice of the stabilization parameter $\eta_{K,e} > 0$ as well as the length parameter $h_{K,e}$ for $e \in \partial K$ is essential to obtain reasonable numerical solutions. In the present isotropic case, we specify a common positive constant η_0 and choose them as follows :

$$\eta_{K,e} = \eta_0 E t, \quad h_{K,e} = |e|. \quad (28)$$

We numerically tested various values of η_0 , and the range $2 \leq \eta_0 \leq 10$ appears to be appropriate in many cases. For coarse meshes, smaller values of η_0 in this range may be preferable so long as the numerical stability is assured. On the other hand, the choice $\eta_0 < 2$ may cause numerical instability, and the one $\eta_0 > 10$ may give too stiff results. Especially, combination of large m and η_0 yields very poor results, although improvement can be still achieved by mesh refinement.

5. NUMERICAL RESULTS

We give some numerical results obtained by the present linear discontinuous Galerkin FEM. We omit the results for the triangular element, which gives the same results as the conventional linear triangular element at least for the problems below.

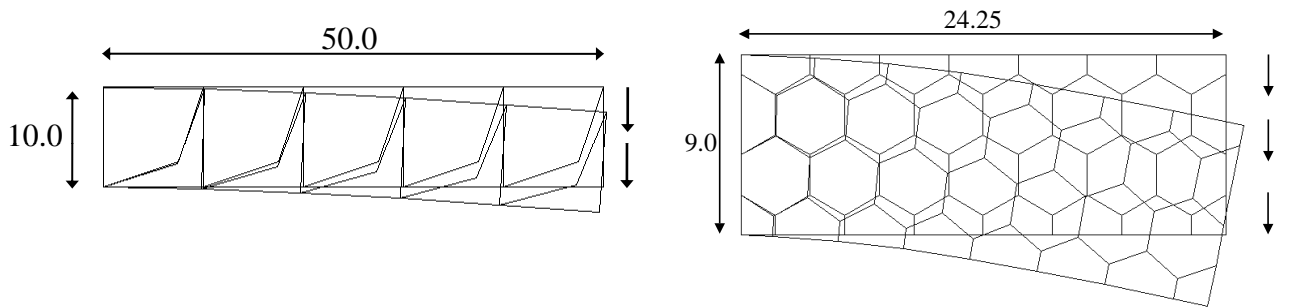


Fig. 2 Meshes and deformed shapes for the cantilever beam problems

5.1 Cantilever problems

Two types of cantilever beams of thin rectangular plate shape subjected to uniform vertical tip loading is analyzed by our approach with polygonal elements of variable m . As is well known, the present problems exhibit severe shear locking phenomena⁴⁾, so that they may be effective to see the performance of various finite element models.

The first case is the use of square cells composed of pairs of convex and non-convex quadrilateral elements, while the second is the mixed use of quadrilateral, pentagonal and hexagonal elements. Examples of coarse meshes with calculated deformed shapes are shown in Fig. 2 for $\eta_0 = 2$, $E = 10000.0$, $\nu = 0.3$ and $t = 1.0$. In addition, the planar plate sizes are: (width, length) = (10, 50), (9.0, 24.25) for the first and second cases, respectively.

For the first problem, we tested meshes with 1×5 , 4×20 and 10×50 square cells for $\eta_0 = 2, 5, 10$. The mesh in Fig. 2 corresponds to the coarse one (1×5), while the deformed meshes for the moderate (4×20) and fine (10×50) cases are shown in Fig. 3. Table 1 for the first case shows the calculated vertical tip displacements normalized by the Timoshenko beam theory⁹⁾ with the shear correction factor $5/6$. Each tip displacement is the one averaged in the vertical (y) direction. We can see that the results depend strongly on η_0 when the mesh is coarse, but they can be improved and converge to the exact value as the mesh is refined.

In the second case, we also tested various η_0 and meshes. The results are, however, more or less similar to those of the first case, so we only show the calculated vertical tip displacements for several η_0 in Table 1 as the second case for the mesh in the right-hand side of Fig. 2.

5.2 Square plate with a circular hole

We also consider a square plate with a central circular hole subjected to uniform end loading in x -direction, see Fig. 4. The dimensions and material properties are: $L = 400.0$, $r = 25.0$, $E = 21000.0$, $\nu = 0.3$, $t = 1.0$, where L is the side length and r the hole radius.

We tested two meshes shown in Fig. 5, and the obtained deformed shape for $\eta_0 = 2$ are illustrated in Fig. 6. For these meshes, we also tested several values of η_0 in the range $2 \leq \eta_0 \leq 10$, but the results are essentially the same in the graphical level and are omitted here.

Moreover, the normal stress σ_x along the y -axis is calculated for the fine mesh and compared with the corresponding analytical solution for the infinite plate¹⁰⁾. Fig. 7 shows the results for $\eta_0 = 2$ together with those based on the above analytical solution. We also tested the classical bilinear quadrilateral element⁴⁾ for the same meshes, but the results are almost the same as the present ones in the graph. The coincidence appears to be generally good, and the present linear quadrilateral element can give results comparable to the classical bilinear element.

6. CONCLUDING REMARKS

We have proposed a discontinuous Galerkin FEM of two-field hybrid displacement type for linear plane stress problems, and presented a formulation for polygonal finite elements with linear approximate displacement fields. Furthermore, we gave numerical results to show the

Table 1: Calculated tip displacements normalized by the Timoshenko beam solutions

case	first			second
mesh	coarse	moderate	fine	coarse only
$\eta_0 = 2$	0.474	0.936	0.997	0.933
$\eta_0 = 5$	0.328	0.885	0.987	0.788
$\eta_0 = 10$	0.204	0.789	0.965	0.635

validity of our approach. In particular, it turned out that even non-convex elements and m -polygonal ones with $m \geq 5$ are available, if the stabilization parameter is carefully chosen. At present, we consider only the linear polygonal elements, since our modest concern is to see the validity of our idea. However, we will test higher order polynomial approximations and three-dimensional problems to demonstrate practical effectiveness of our approach. Theoretical analysis based on functional analysis is also important and to be performed in future works.

This work is partially supported by JSPS, Grant-in Aid for Scientific Research (C) 19540115.

REFERENCES

- 1) D. N. Arnold, F. Brezzi, B. Cockburn, L. D. Marini, *Unified analysis of discontinuous Galerkin methods for elliptic problems*, SIAM J. Numer. Anal., **39** (2002) 1749-1779.
- 2) B. Q. Li, “Discontinuous Finite Elements in Fluid Dynamics and Heat Transfer”, Springer, 2006.
- 3) S. C. Brenner, L. R. Scott, “The Mathematical Theory of Finite Element Methods”, Springer, 2008.
- 4) T. H. H. Pian, C.-C. Wu, “Hybrid and Incompatible Finite Element Methods”, Chapman & Hall, 2005.
- 5) P. Tong, *New displacement hybrid finite element models for solid continua*, Int. J. Num. Meth. Eng., **1** (1969) 101-122.
- 6) F. Kikuchi, Y. Ando, *A new variational functional for the finite-element method and its application to plate and shell problems*, Nucl. Eng. Des., **21** (1972) 95-113.
- 7) F. Kikuchi, Y. Ando, *Some finite element solutions for plate bending problems by simplified hybrid displacement method*, Nucl. Eng. Des., **23** (1972) 155-178.
- 8) R. Mihara, N. Takeuchi, *The three dimension models development by using linear displacement fields in HPM*, presented at APCOM’07 in conj. with EPMESC XI, Dec. 3-6, 2007, Kyoto, Japan.
- 9) K. Washizu, “Variational Methods in Elasticity and Plasticity”, 3rd ed., Pergamon, 1982.
- 10) S. P. Timoshenko and J. N. Goodier, “Theory of Elasticity”, 3rd ed., McGraw-Hill, 1970.

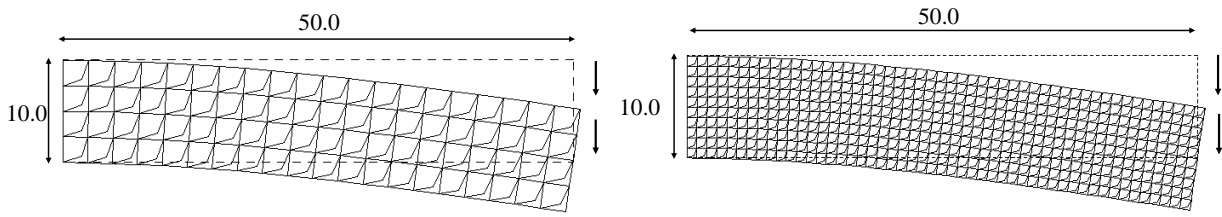


Fig. 3 Meshes and deformed shapes for the first cantilever beam problem : moderate and fine meshes

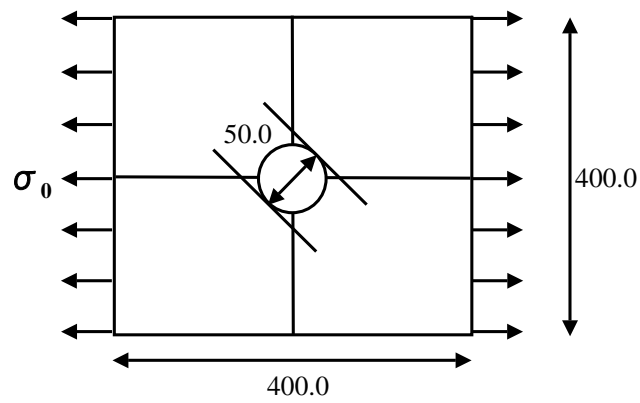


Fig. 4 Square plate with a central circular hole

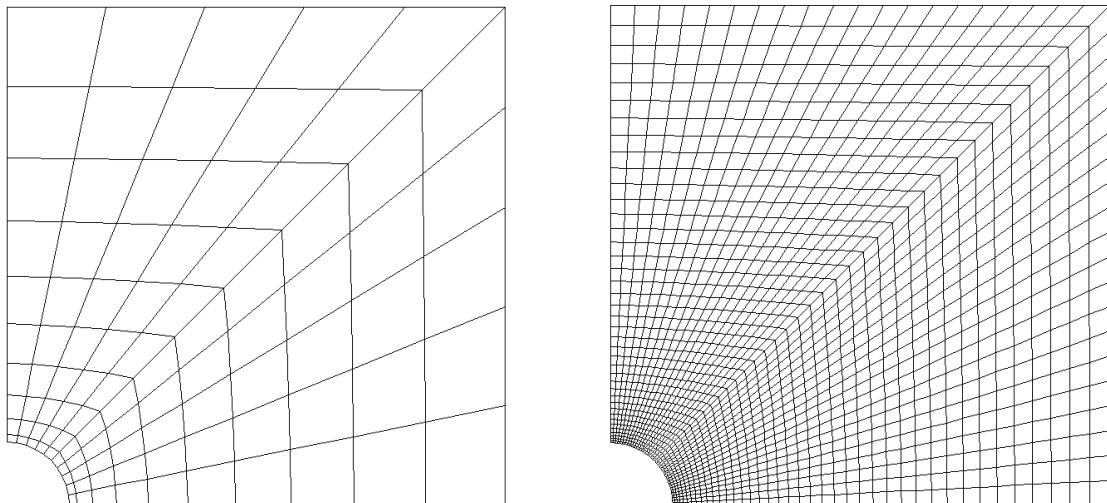


Fig. 5 Meshes for the square plate with a hole : coarse and fine meshes

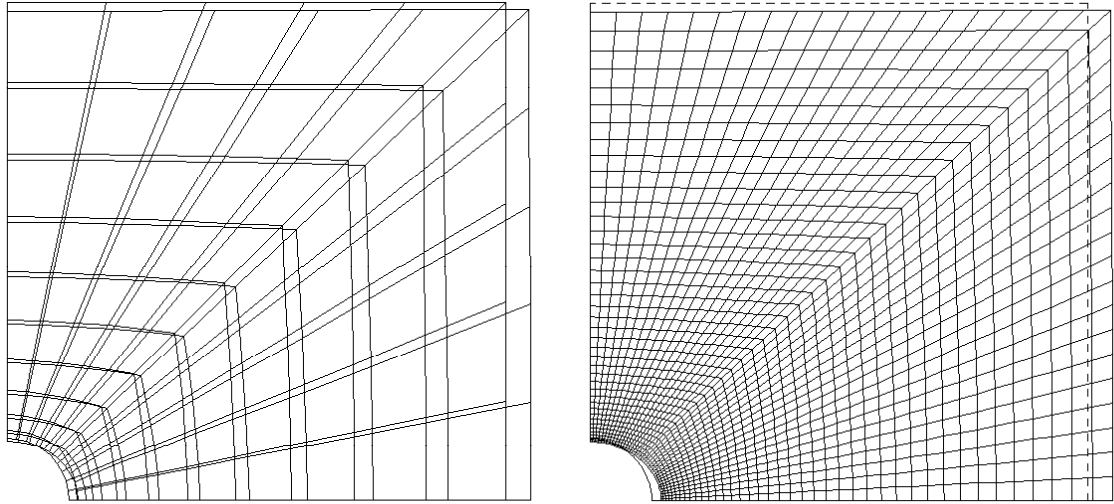


Fig. 6 Calculated deformed forms of the square plate with a hole

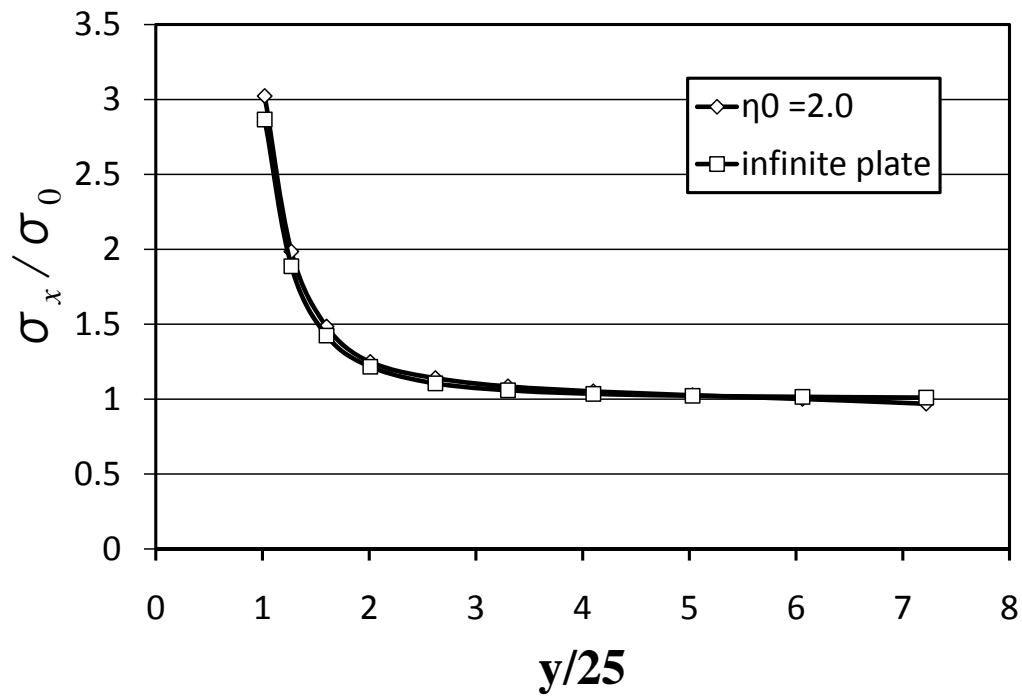


Fig. 7 Distribution of σ_x along vertical centerline (y -axis)

UTMS

- 2008–10 Takashi Tsuboi: *On the uniform perfectness of diffeomorphism groups.*
- 2008–11 Takashi Tsuboi: *On the simplicity of the group of contactomorphisms.*
- 2008–12 Hajime Fujita, Mikio Furuta and Takahiko Yoshida: *Acyclic polarizations and localization of Riemann-Roch numbers I.*
- 2008–13 Rolci Cipolatti and Masahiro Yamamoto: *Inverse hyperbolic problem by a finite time of observations with arbitrary initial values.*
- 2008–14 Yoshifumi Matsuda: *Groups of real analytic diffeomorphisms of the circle with a finite image under the rotation number function.*
- 2008–15 Shoichi Kaji: *The (\mathfrak{g}, K) -module structures of the principal series representations of $SL(4, R)$.*
- 2008–16 G. Bayarmagnai: *The (\mathfrak{g}, K) -module structures of principal series of $SU(2,2)$.*
- 2008–17 Takashi Tsuboi: *On the group of real analytic diffeomorphisms.*
- 2008–18 Takefumi Igarashi and Noriaki Umeda: *Nonexistence of global solutions in time for reaction-diffusion systems with inhomogeneous terms in cones.*
- 2008–19 Oleg Yu. Imanouilov, Gunther Uhlmann, and Masahiro Yamamoto: *Partial data for the Calderón problem in two dimensions.*
- 2008–20 Xuefeng Liu and Fumio Kikuchi: *Analysis and estimation of error constants for P_0 and P_1 interpolations over triangular finite elements.*
- 2008–21 Fumio Kikuchi, Keizo Ishii and Issei Oikawa: *Discontinuous Galerkin FEM of Hybrid displacement type – Development of polygonal elements –.*

The Graduate School of Mathematical Sciences was established in the University of Tokyo in April, 1992. Formerly there were two departments of mathematics in the University of Tokyo: one in the Faculty of Science and the other in the College of Arts and Sciences. All faculty members of these two departments have moved to the new graduate school, as well as several members of the Department of Pure and Applied Sciences in the College of Arts and Sciences. In January, 1993, the preprint series of the former two departments of mathematics were unified as the Preprint Series of the Graduate School of Mathematical Sciences, The University of Tokyo. For the information about the preprint series, please write to the preprint series office.

ADDRESS:

Graduate School of Mathematical Sciences, The University of Tokyo
3–8–1 Komaba Meguro-ku, Tokyo 153-8914, JAPAN
TEL +81-3-5465-7001 FAX +81-3-5465-7012